energy&fuels

Subscriber access provided by University of Newcastle, Australia

Article

Properties of carbon dioxide foam stabilized by hydrophilic nanoparticles and hexadecyl trimethyl ammonium bromide

Songyan Li, Chenyu Qiao, Zhaomin Li, and Silagi Wanambwa

Energy Fuels, **Just Accepted Manuscript** • DOI: 10.1021/acs.energyfuels.6b03130 • Publication Date (Web): 18 Jan 2017

Properties of carbon dioxide foam stabilized by hydrophilic nanoparticles and hexadecyl trimethyl ammonium bromide

Songyan Li*, Chenyu Qiao, Zhaomin Li*, Silagi Wanambwa

College of Petroleum Engineering, China University of Petroleum (East China), 266580, China

ABSTRACT: Nanoparticles can improve the stability of CO_2 foam and increase oil recovery during CO_2 flooding in reservoirs. The synergistic effect of hydrophilic SiO_2 nanoparticles and hexadecyl trimethyl ammonium bromide (CTAB) on CO_2 foam stability was examined in this study. Experimental results show that the synergistic effect requires a CTAB/SiO_2 concentration ratio of 0.02 to 0.07, with 0.033 representing the best concentration ratio. With the increase in the concentration ratio, the synergistic stabilization effect of CTAB/SiO_2 dispersion first increases and then decreases. In the monolayer adsorption stage (concentration ratio from 0.02 to 0.033), when the hydrophobicity of SiO_2 nanoparticles increases with the concentration ratio, the nanoparticles tend to adsorb on the gas-liquid interface, and the stability of CO_2 foam increases. In the double-layer adsorption stage (concentration from 0.033 to 0.07), when the hydrophobicity of SiO_2 nanoparticles decreases with an increase in the concentration ratio, the nanoparticles tend to exist in the bulk phase, and the stability of CO_2 foam decreases. The CTAB/SiO_2 dispersion stabilizes CO_2 foam via three mechanisms: decreasing the coarsening of CO_2 bubbles, improving interfacial properties, and reducing liquid discharge. CTAB/SiO_2 foam can greatly improve oil recovery efficiency compared with water flooding. Experimental results provide theoretical support for improving CO_2 foam flooding under reservoir conditions.

KEYWORDS: hydrophilic nanoparticles, synergistic effect, CO_2 foam, stabilization, oil recovery

1. INTRODUCTION

With the international community's increasing emphasis on the reduction of CO_2 emissions, CO_2 geological storage has become a popular technology area.[1] CO_2 can dissolve in crude oil and play a special role in reducing the viscosity and expanding the volume of crude oil under reservoir conditions;[2-4] therefore, CO_2 flooding has become an important method for enhancing oil recovery.[5] However, CO_2 has much greater mobility than crude oil, and gas channeling results in a lower volumetric sweep efficiency.[6] A foam is a dispersion system with high apparent viscosity and the characteristic of blocking formations with high permeability, and foams have yielded good results in CO_2 mobility control.[7] Nevertheless, due to the characteristics of CO_2 and the high-temperature and high-salinity environment of reservoirs, CO_2 foams cannot be stable for long periods in formations, making it difficult to meet production requirements.

Nanoparticles have unique surface characteristics. Nanoparticles with a certain hydrophobicity can adsorb onto liquid-liquid or gas-liquid interfaces to improve the stability of emulsions or foams.[8] As one of the most commonly used nanomaterials, SiO_2 nanoparticles have numerous advantages, such as a widespread source, moderate price, mature technology, and stable properties. SiO_2 nanoparticles with excellent performance in adsorption, dispersion, surface energy, electrology and thermodynamics are widely used in construction, medicine, electronics and other fields and have become an important production and research material with excellent prospects for development.[9-11]

In recent years, the surface performance of SiO_2 nanoparticles and its interaction with surfactant molecules have been studied intensively. Many scholars have achieved groundbreaking results. Bi et al. immersed SiO_2 flakes in solutions with different CTAB concentrations and measured the change in contact angle as well as the thickness of the adsorption layer on SiO_2 flakes after adsorption equilibrium.[12] Through this method, they monitored the wettability of SiO_2 flakes with increasing CTAB concentration and observed the formation of a bilayer of CTAB molecules on the surface of SiO_2. Tyrode et al. and Somasundaran et al. also studied the adsorption of CTAB on the surface of hydrophilic silica through optical methods.[13-14] According to their experiment results, the adsorption isotherm of CTAB is highly similar to the two-step adsorption model. They did not observe any asymmetry in the first plateau of the CTAB adsorption isotherm via sum-frequency spectroscopy (SFS); therefore, they ruled out the possibility that hemimicelle partial monolayers form in this region. However, due to the limited sensitivity of their instruments, they did not attain a sufficient level of detail in that concentration region. Santini et al. investigated the properties of the dispersion with hydrophilic silica nanoparticles and CTAB.[15] According to their results, CTAB molecules form an unsaturated monolayer structure in a relatively high concentration and covers silica nanoparticles, which make hydrophilic particles become more hydrophobic. The change in wettability properties causes silica nanoparticles to be transferred from the bulk to the air-liquid interface. Furthermore, by virtue of the exchange of CTAB molecules between the silica surface and liquid, the adsorbed layer reorganizes and leads to the formation of irregular solid structures at the air-liquid interface. Solid structures change the interfacial rheological properties, which can stabilize foams and emulsions.[16]

Several researchers have presented results concerning the stabilization of foams by nanoparticles and surfactants. Zhang et al. studied the synergistic effect between Laponite particles and cationic surfactant CTAB on stabilizing aqueous foams. Experimental results

show that foams prepared using a Laponite/CTAB dispersion are more stable than foams prepared using a pure CTAB solution.[17] When the concentration of Laponite particles is fixed, the foam stability first increases and then decreases with the increase in CTAB concentration and reaches a maximum of 1.7 cec. There are two mechanisms that can enhance foam stability. First, particles with partial hydrophobicity adsorb onto the air-liquid surface; second, Laponite particles in the bulk form a spatial structure that can increase the viscosity of the particles/surfactant dispersion.[17-21] Liu et al. indicated that the crux of the synergistic effect on the stabilization of foams between nanoparticles and surfactants is the adsorption of modified nanoparticles onto the gas-liquid surface.[22] According to their results, the adsorption of alkyltrimethylammonium bromides onto Laponite obeys a four-region model. The stability of foams reaches a maximum at an intermediate surfactant concentration, when surfactant molecules form a monolayer structure on the surface of particles, and thus particles attain the best hydrophobicity. Moreover, surfactants with longer hydrocarbon chains can form final adsorption conformations at lower concentrations. Worthen et al. found that the addition of SiO_2 nanoparticles can greatly increase the apparent viscosity of foams, which reinforces the stability of foams.[23]

To date, studies on stabilizing foams with SiO_2 nanoparticles have mainly concentrated on hydrophobic nanoparticles, and less attention has been paid to hydrophilic nanoparticles. Experimental results pertaining to the stabilization of CO_2 foams by hydrophilic SiO_2 nanoparticles are limited. Compared with hydrophobic SiO_2 nanoparticles, hydrophilic SiO_2 nanoparticles are less expensive and disperse better in water. In this study, the synergistic effects on improving CO_2 foams' stability by hydrophilic SiO_2 nanoparticles and the cationic surfactant CTAB were evaluated, and the mechanisms of foam stabilization were researched based on the conformations of CTAB molecules adsorbed on nanoparticles. The results are meaningful for the application of CO_2 foam flooding for enhanced oil recovery (EOR).

2. EXPERIMENTAL METHODS

2.1 Materials

CTAB purchased from Aladdin Industrial Corporation (USA) with a purity greater than 99.0 % was used as a surfactant for a CO_2 foam. CTAB is a common cationic surfactant with a simple molecular structure. Deionized water with a resistivity ranging from 17 MΩ.cm to 18.2 MΩ.cm served as the liquid phase in all the experiments. CO_2 was supplied by Tianyuan Gas Company (China) with a purity greater than 99.9 %. Hydrophilic SiO_2 nanoparticles of the type HDK N20 with a purity greater than 99.8 % were purchased from Germany Wacker

Chemical Co., Ltd. The average nanoparticle diameter was 40 nm. The contact angle of SiO_2 nanoparticles with pure water is 38.63 °.

The original heavy crude oil was collected from the Shengli oilfield in Shandong, China. The obtained heavy crude oil was cleaned by using a centrifuge to remove any sands and brine. The density and viscosity of the cleaned heavy crude oil were measured to be 835.2 kg/m^3 by using a densitometer (DMA 512P, Anton Paar, Austria) and 89.1 mPa.s by using a rheometer (MCR302, Anton Paar, Austria) at the atmospheric pressure and 50.0 °C.

2.2 Apparatus

A balance (Model ML, Mettler Toledo, Switzerland, full scale of 120 g, accuracy of 0.001 g) was used to weigh the surfactant and nanoparticles. An ultrasonic dispersion instrument (Model TJS-3000, Hangzhou Ultrasonic Equipment Co., ltd., China) and a magnetic agitator (Model HJ-4, stirring speed less than 1400 rpm, Changzhou Electric Appliance Co., ltd., China) were used to disperse SiO_2 in the surfactant solution. The interfacial viscoelastic modulus and surface tension of a pure CTAB solution and a CTAB/SiO_2 dispersion were determined by a drop shape tensiometer (Tracker-H, Teclis, France, full scale of 20.0 MPa and 200 °C).[24] A viscometer (Model DV-III, Brookfield, America, accuracy of ±1%, reproducibility of ±0.2%) was used to measure the viscosities of the liquids. A dynamic light scattering instrument (Model Zetasizer nano ZS, particle size range of 3 nm to 100 μm, precision of 0.12 μm.cm/V.s, Malvern instruments Co., Ltd., British) was utilized to test the ζ potential of the CTAB/SiO_2 dispersion. Foams were prepared using a blender (Model GJ-3S, Qingdao Senxin Machinery Equipment Co., Ltd., China). The performances of the foams were determined using a FoamScan instrument (Model HT, Teclis, France, full scale of 0.8 MPa and 120 °C), which can monitor the CO_2 foam volume, foam stability, liquid holdup in CO_2 bubbles, and bubble structure.[25-26]

The experimental apparatus for visual flooding is shown in Figure 1, and microscopic model built of toughened glass has been used in the experiments. The microscopic model is made according to the core sample collected from Shengli oilfield in Shandong, China. First, the core sample is ground into thin slice, and the structure of the porous media is recorded by photography. Then the laser etching method is used to make the microscopic model on two pieces of tempering glass according to the structure of the core slice. Thirdly, the two pieces of glass sticks together under 600 ^oC in a muffle roaster. Therefore, the microscopic model used in the visual flooding experiment can stand for the real formation. Flow of CO_2 foam in the microscopic model is almost the same as that in the actual reservoir. The model has a porous media area of 40 mm × 40 mm, and the depth and width of the flow channel are 60 μm

and 80 μm, respectively. The microscopic model is placed in a holder with a pressure of less than 20 MPa and temperature less than 100 °C. A video of the foam flow in the microscopic model has been recorded by a digital microscopic imaging system, which can be used for flow mechanism analysis. There is a foam generator in Figure 1 to mix the CO_2 and CTAB/SiO_2 dispersion before they flow into the microscopic model, which is usually used in foam flooding experiments. The foam generator is actually a small sandpack with length of 10.00 cm and inner diameter of 1.50 cm, filled with sand of 20-40 mesh. It can generate uniform and stable foam for flooding crude oil.

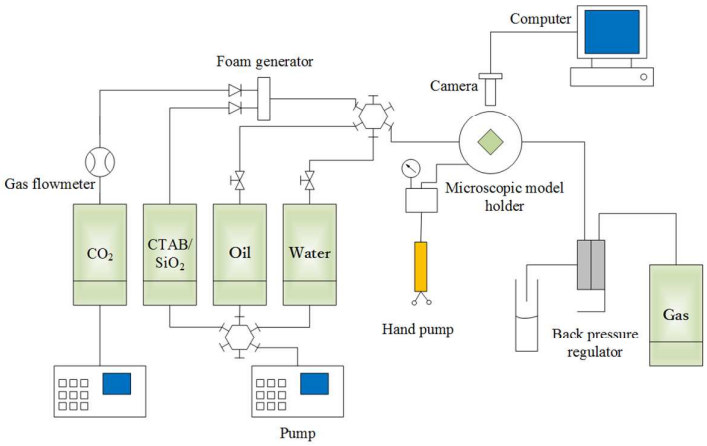

Figure. 1 The experimental apparatus for visual flooding.

2.3 Experimental methods

2.3.1 CTAB/SiO_2 dispersion preparation

First, a certain amount of SiO_2 nanoparticles was added to distilled water and dispersed using an ultrasonic dispersive spectrometer for 10 min to obtain a uniform SiO_2 dispersion. Then, a certain amount of CTAB was added to the SiO_2 dispersion and was dispersed by a magnetic agitator for 3 min, forming a uniform CTAB/SiO_2 dispersion. The dispersion was kept static for 24 h at room temperature to reach the adsorption equilibrium of the surfactant CTAB on the surface of the SiO_2 nanoparticles.

2.3.2 Surface tension and interfacial viscoelastic modulus testing

The surface tension and interfacial viscoelastic modulus of the CTAB solution or CTAB/SiO_2 dispersion with CO_2 were tested by the pendant drop method using a Tracker-H tensiometer. The volume of the liquid drop was 5 μL, the oscillation frequency was 0.1 Hz, and the amplitude was 1 μL. Details about the tensiometer and pendent drop method can be found elsewhere.[27]

2.3.3 Determination of ζ potential of CTAB/SiO_2 dispersion

The nanoparticles in the CTAB/SiO_2 dispersion with a diameter greater than 200 nm were

removed by a filter. Then, the ζ potentials of CTAB/SiO_2 dispersions of different concentrations were determined by dynamic light scattering. The ζ potentials were measured five times, and the average values were obtained.

2.3.4 CTAB/SiO_2 foam evaluation

The properties of the CTAB/SiO_2 foam at room temperature were tested using a blender, as in previous studies.[8] The liquid holdup in the CTAB/SiO_2 foam was test by the FoamScan instrument. A 50 ml dispersion was injected into the sample barrel, and CO_2 gas was injected at a volume flow rate of 200 ml/min to generate CO_2 foam until the foam volume reached 200 ml. Then, the foam volume, foam stability, liquid holdup in CO_2 bubbles, and bubble structure were determined.

2.3.5 Visual flooding experiment

The flow of the CTAB/SiO_2 foam in the visual porous media was observed using the apparatus shown in Figure 1. First, water was saturated with a flow rate of 0.1 ml/min, and crude oil was saturated with a flow rate of 0.05 ml/min. Water flooding was then performed at a flow rate of 0.1 ml/min until the water cut of the produced liquid reached 80%. Finally, the CTAB/SiO_2 foam was injected at flow rate of 0.1 ml/min for 3 porous volume (PV) of the microscopic model. A video of the foam flow through the microscopic model was recorded by a digital microscopic imaging system.

3. RESULTS AND DISCUSSION

3.1 CTAB/SiO_2 foam evaluation

Experimental results for the CO_2 foam generated by a pure CTAB solution are shown in Figure 2. The figure shows that the foam volume did not undergo any appreciable change with the increase in the CTAB concentration, which was maintained at approximately 320 ml. The reason is that the foam volume mainly depends on the surface tension of the surfactant solution and CO_2 gas.[28] When the surfactant concentration is above the critical micelle concentration (CMC), the rising surfactant concentration will not alter the surface tension significantly. According to the literature, the CMC of CTAB is 8.9×10^{-4} mol/l.[29] The CTAB concentrations used in this study were much greater than that value; therefore, the bubble volume did not change appreciably with the increase in the CTAB concentration.

With the increase in the CTAB concentration, the half-life of the CTAB foam increases first. When the CTAB concentration reaches 0.3 wt%, the half-life nearly levels off. At a low CTAB concentration, the adsorption of the surfactant onto the gas-liquid interface does not reach saturation. With the increase in the CTAB concentration, the adsorption of more CTAB

molecules onto the gas-liquid interface can greatly improve the film strength, viscoelastic property, and foam stability.[30] When the CTAB molecules on the interface reach saturation, more CTAB molecules will form micelles in solution, which cannot improve the foam stability further.

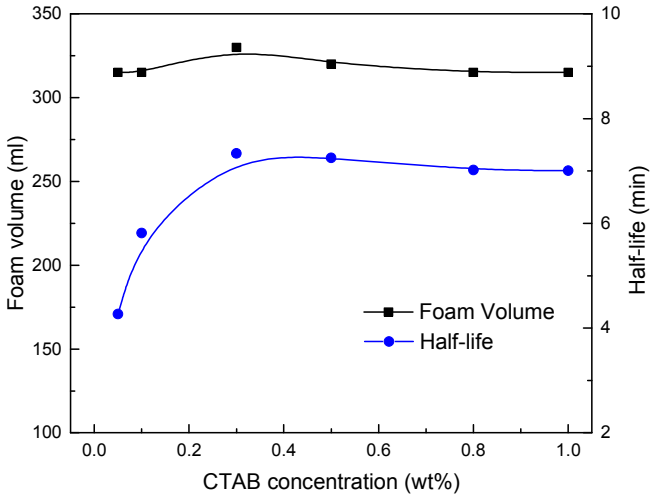

Figure. 2 The effect of CTAB concentration on CO_2 foam properties.

The experimental results obtained for the CO_2 foam generated by the CTAB/SiO_2 dispersion are shown in Figure 3. CTAB which is cationic has been selected to stabilize CO_2 foam with hydrophilic nanoparticles. The original contact angle of the SiO_2 nanoparticles with pure water is 38.63 °, however, the best value for stabilizing foam is from 60 ° to 90 °. The surface of the SiO_2 nanoparticles shows a negative potential,[31] and the CTA^+ cations can adsorb onto the surface of SiO_2 nanoparticles at low or medium concentrations of CTAB as a monolayer via electrostatic interactions, which can increase the contact angle of the SiO_2 nanoparticles with pure water. If it lies in the range of 60 ° to 90 ° with a proper CTAB concentration, the stability of CO_2 foam can be obviously improved. Comparing Figure 3 with Figure 2 reveals that the foaming capability of the CTAB/SiO_2 dispersion was nearly the same as that of the pure CTAB solution. However, when the concentration ratio of CTAB to SiO_2 was increased from 0.02 to 0.07, the dispersion showed a distinct synergistic effect on the stabilization of the CO_2 foam. The peak value of the half-life of the CO_2 foam is approximately seven times that of the pure CTAB solution.

Figure 3 also shows that with the rising concentration ratio of CTAB to SiO_2, the half-life of the CO_2 foam varied significantly. When the CTAB/SiO_2 concentration ratio was less than 0.02 (region I in Figure 3), the stability of the CO_2 foam was weak, and no synergistic effect was observed. When the concentration ratio was increased from 0.02 to 0.07, the dispersion

showed a strong synergistic effect (region II in Figure 3). The half-life reached a peak value at a CTAB/SiO_2 concentration ratio of 0.033. When the concentration ratio was greater than 0.07 (range III in Figure 3), the half-life of the CO_2 foam reached relatively low values, showing no obvious synergistic effect. The stability of the CTAB/SiO_2 foam was nearly the same as that of the CTAB foam at the same concentration.

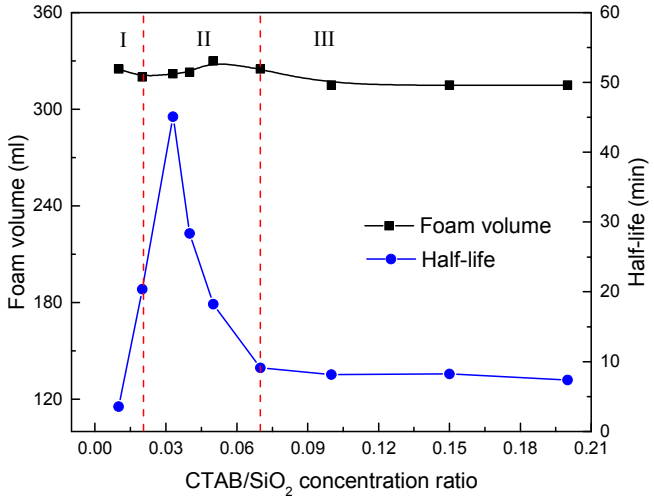

Figure. 3 The effect of CTAB/SiO_2 concentration ratio on CO_2 foam properties.

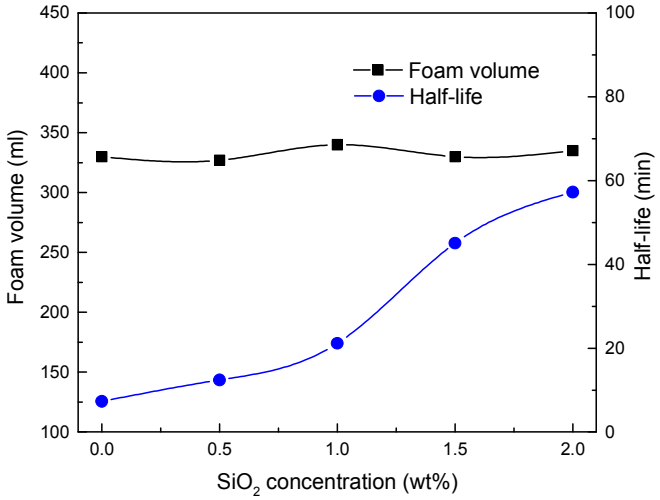

Figure. 4 The effect of SiO_2 concentration on CO_2 foam properties.

The best performance of the CO_2 foams formed by CTAB/SiO_2 dispersions with different SiO_2 concentrations is shown in Figure 4. The results show that the addition of SiO_2 nanoparticles to the surfactant solution had no effect on the foaming capability of the CO_2 foam, and the foam volumes remained nearly constant at 330 ml. With the increase in the SiO_2 concentration, the stability of the CO_2 foam changed significantly. In particular, when the concentration of SiO_2 was increased from 1.0 wt% to 2.0 wt%, the half-life rose quickly.

The optimum SiO_2 nanoparticle concentration was 1.5 wt%.

3.2 Synergistic stabilizing effect of CTAB and SiO_2

3.2.1 Modulating the nanoparticles' adsorbing position

The main synergistic stabilizing effect of CTAB and SiO_2 on CO_2 foam is the adsorption of SiO_2 nanoparticles modified by CTAB on the gas-liquid interface. Only SiO_2 nanoparticles adsorbed on the gas-liquid interface can effectively improve the stability of the CO_2 foam. The modification of SiO_2 nanoparticles at different CTAB concentrations is shown in Figure 5. When the pH value of the solution is greater than 2.5, the surface of the SiO_2 nanoparticles shows a negative potential.[31] The pH value of the CTAB/SiO_2 dispersion used in this study ranged from 7 to 8; therefore, the potential of the SiO_2 nanoparticles was negative. As shown in Figure 5, the CTA^+ cations can adsorb onto the surface of SiO_2 nanoparticles at low or medium concentrations of CTAB as a monolayer via electrostatic interactions. At high concentrations of CTAB, they can adsorb onto the SiO_2 surface as a double-layer due to hydrophobic associative interactions along the carbon chain.

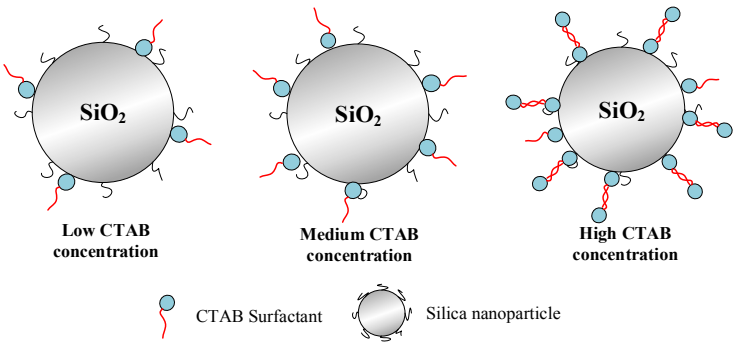

Figure. 5 The adsorption of CTAB surfactant on SiO_2 nanoparticles in water.

The ζ potentials of CTAB/SiO_2 dispersions under different concentration ratios are illustrated in Figure 6. The states of the CTAB/SiO_2 dispersions are shown in Figure 7, which corresponds well with the relationships shown in Figure 6. At low CTAB concentrations, few CTA^+ ions adsorbed on the surface of the SiO_2 nanoparticles. The ζ potential was negative and showed a high absolute value. The electrostatic repulsion force among nanoparticles was strong, and the nanoparticles were difficult to precipitate. The dispersion showed a uniform state (shown in Figure 7a). With the increase in the CTAB concentration, more CTA^+ ions adsorbed onto the surface of the SiO_2 nanoparticles, and the ζ potential of the dispersion gradually increased to zero. The electrostatic repulsion force among nanoparticles became weak, and some of the nanoparticles precipitated (Figure 7b). With a further increase in the CTAB concentration, even more CTA^+ ions adsorbed onto the surface of nanoparticles, forming a double-layer as shown in Figure 5. The ζ potential of the dispersion increased from

negative to positive, and the absolute value increased to a high value, as shown in Figure 6. The electrostatic repulsion force among SiO_2 nanoparticles was reinforced, and nanoparticles dispersed in the CTAB solution (shown in Figure 7c-f). When the CTAB molecules that adsorbed onto the SiO_2 nanoparticle surface reached their final conformation, the ζ potential reached a high value of 35 mV, and the dispersion maintained a uniform and stable state. The evolution of the adsorption conformation of SiO_2 nanoparticles is similar to that shown in Figure 5.

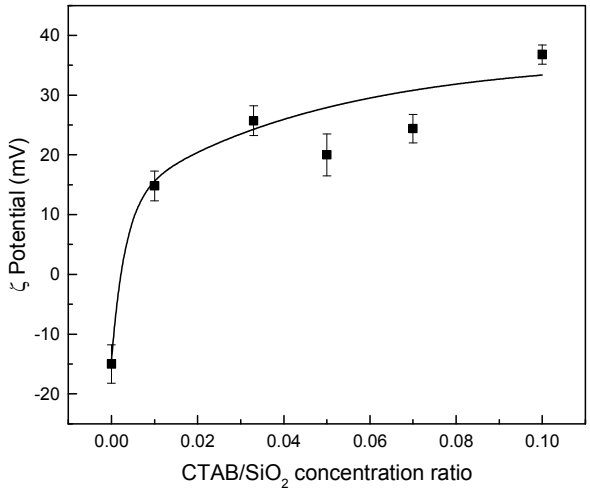

Figure. 6 The ζ potential at different CTAB/SiO_2 concentration ratios.

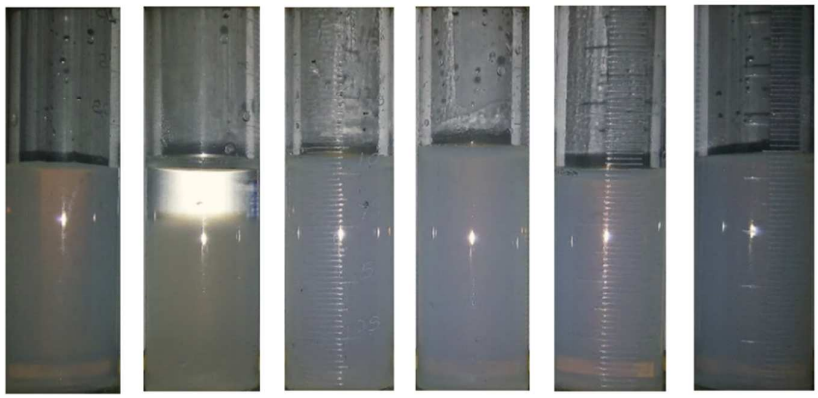

a **b** **c** **d** **e** **f**

(I)

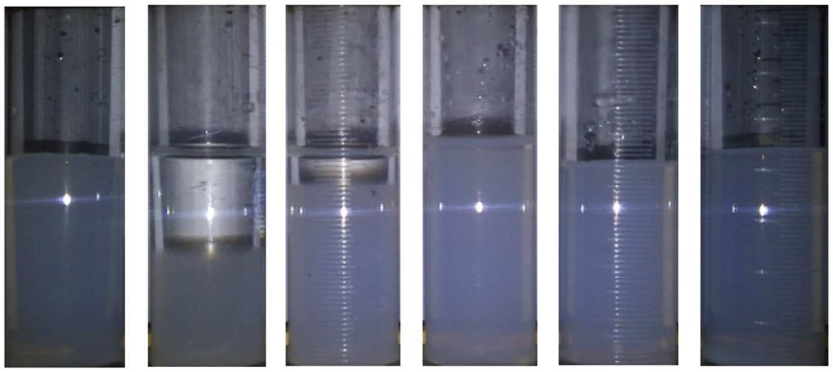

a b c d e f

(II)

Figure. 7 The settling time for CTAB/SiO_2 dispersion (I) is 24 h, and that for (II) is 48 h. The CTAB/SiO_2 concentration ratios from left to right are 0, 0.01, 0.033, 0.05, 0.07 and 0.1.

The distribution of SiO_2 nanoparticles in the bubble film at different CTAB/SiO_2 concentration ratios is shown in Figure 8, which corresponds well with the experimental results shown in Figure 3. As shown in Figure 8, the CTAB concentration in region A was very low, and the amount of CTAB molecules adsorbed onto the surface of SiO_2 nanoparticles was small. The surface of the nanoparticles was hydrophilic, and the nanoparticles distributed mainly in the continuous liquid phase (bulk phase). The properties of the CTAB/SiO_2 dispersion were nearly the same as those of the pure CTAB solution for stabilizing the CO_2 foam, and no synergistic effect was observed. The CTAB concentration in region B was higher than that in region A. The CTAB molecules began to adsorb onto the surface of the SiO_2 nanoparticles. The hydrophilic ends of CTAB interacted electrostatically with the surface of the nanoparticles, and the hydrophobic ends were exposed, forming a hydrophobic single layer. Because the adsorption of CTAB molecules enhances the hydrophobicity of SiO_2 nanoparticles, the distribution gradually moved from the liquid to the gas-liquid interface. The CTAB/SiO_2 dispersion began to show synergistic effects in stabilizing the CO_2 foam (related to region I in Figure 3).

The CTAB concentration in region C was in the optimal range. In this region, a moderate amount of CTAB molecules adsorbed onto the surface of SiO_2 nanoparticles, forming a tight single adsorption layer or an incomplete double adsorption layer. The SiO_2 nanoparticles showed strong hydrophobicity. At this time, a large number of SiO_2 nanoparticles adsorbed onto the gas-liquid interface, demonstrating a strong synergistic effect in stabilizing the CO_2 foam and greatly improving the stability of the CO_2 bubbles (related to region II in Figure 3).

With the further increase in the CTAB concentration in region D of Figure 8, the adsorbed SiO_2 nanoparticles formed a double-layer with the hydrophilic ends facing outwards, which

strengthened the hydrophilicity of the nanoparticles. The nanoparticles gradually moved from the gas-liquid interface back to the bulk phase. At the same time, micelles formed in the dispersion due to the high concentration of CTAB.[17, 22, 31] The stability of the CO_2 foam was strongly inhibited, and the synergistic effect weakened rapidly (related to region III in Figure 3). After the formation of the final adsorption conformation, the foam stability underwent no change with the increase in the CTAB concentration.

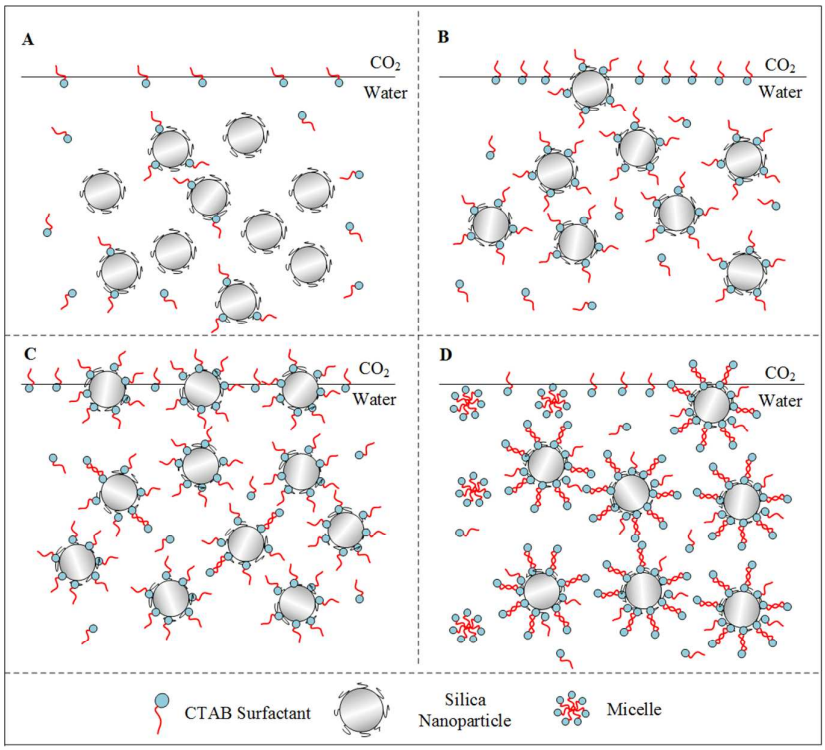

Figure. 8 The adsorption of SiO_2 nanoparticles onto the CO_2-water interface. The CTAB/SiO_2 concentration ratio increases from region A to region D.

The states of the CTAB/SiO_2 foam at different CTAB/SiO_2 concentration ratios are illustrated in Figure 9, which corresponds well with the relationships shown in Figure 8. At low CTAB concentrations, the liquid discharged from the CO_2 foam was turbid, indicating a high percentage of SiO_2 nanoparticles in the bulk phase. The reason is that the SiO_2 nanoparticle surface was more hydrophilic; thus, the nanoparticles were mainly distributed in the continuous liquid phase (related to regions A and B in Figure 8). When the CTAB concentration was moderate, the liquid discharged from the CO_2 foam was clear, and most of the nanoparticles remained at the gas-liquid interface due to high hydrophobicity (related to region C in Figure 8). At higher CTAB concentrations, the liquid discharged from the CO_2 foam became turbid again, and most of the nanoparticles returned to the bulk phase due to the low hydrophobicity (related to region D in Figure 8).

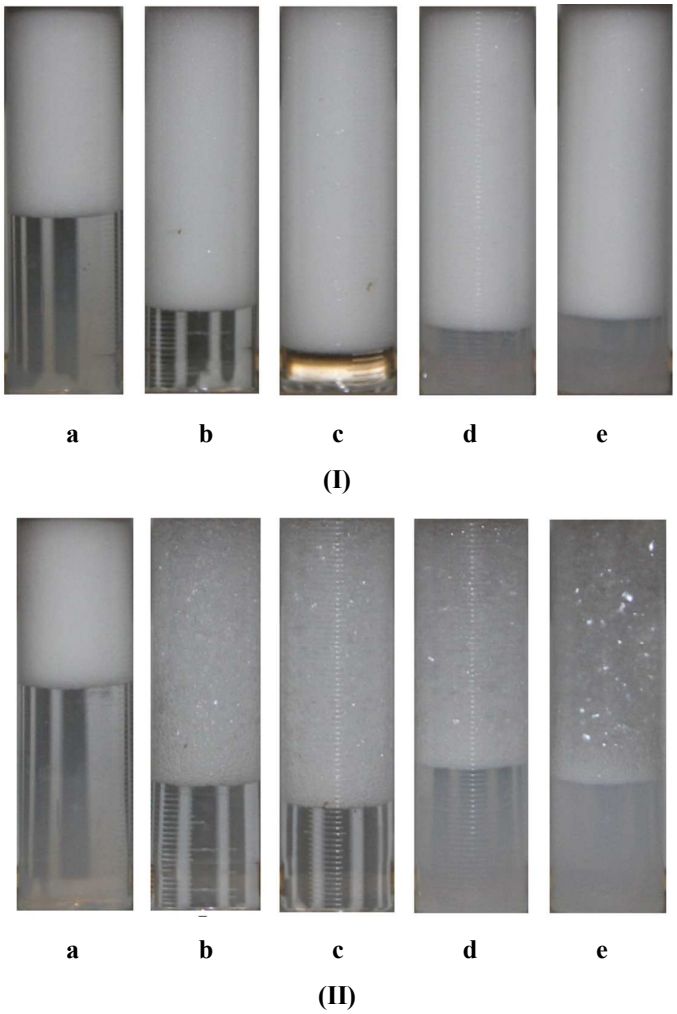

Figure. 9 The settling times for CO_2 foam prepared by CTAB/SiO_2 dispersion were 10 min and 3 h for (I) and (II). The CTAB/SiO_2 concentration ratios from left to right are 0.01, 0.033, 0.05, 0.07 and 0.1.

3.2.2 Decreasing the coarsening of CO_2 foam

According to the Young – Laplace equation, bubbles with a small diameter in a foam have a higher pressure, resulting in greater CO_2 dissolution in a film formed of small bubbles.[32-33] According to Fick's law of diffusion, the CO_2 in bubbles with a small diameter will diffuse gradually into those with a large diameter through the films. Small bubbles become smaller, and large bubbles become larger. This process is called Ostwald ripening or coarsening.[34] Ostwald ripening is one of the main factors leading to the instability of foams. The solubility of CO_2 in water is far greater than that of air or nitrogen; therefore, the effect of Ostwald ripening on CO_2 foam stability is particularly important.

As shown in Figure. 10, some areas of the gas-liquid interface become a gas-solid interface because of the adsorption of SiO_2 nanoparticles. The adsorption of a sufficient number of

nanoparticles onto the gas-liquid interface can greatly reduce the contact area between CO_2 and the liquid, effectively slowing down the diffusion of CO_2 from small bubbles to larger ones. The Ostwald ripening process can be inhibited to some extent, enhancing the stability of the CO_2 foam.

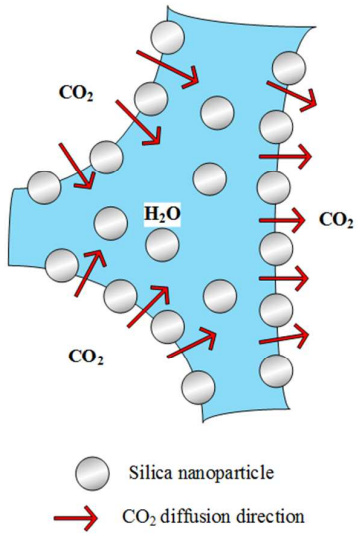

Figure. 10 The reduction of CO_2 foam coarsening by SiO_2 nanoparticles.

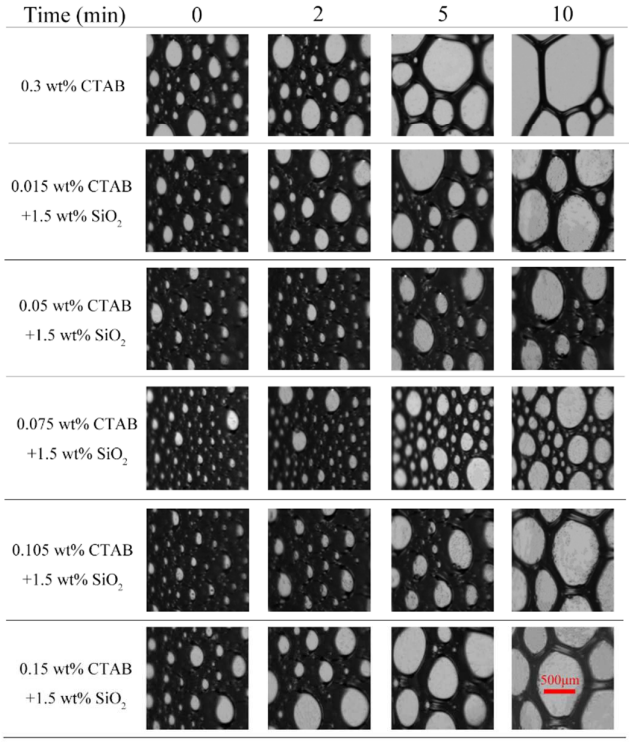

Figure. 11 Micrographs of CO_2 foams with different CTAB/SiO_2 concentration ratios.

Micrographs of CO_2 foams with different CTAB/SiO_2 concentration ratios are presented in Figure 11. The interfaces between the liquid and CO_2 gas phases are distinct in the first row in

Figure 11, at a pure CTAB concentration of 0.3%. However, the interfaces in the other images are slightly blurred because of the adsorption of SiO_2 nanoparticles. The bubble diameters gradually increased over time via Ostwald ripening. The bubbles clearly remained small and the liquid holdup was high at CTAB/SiO_2 concentration ratios ranging from 0.02 to 0.07 in the third and fourth rows in Figure 11. The experimental results prove the theory illustrated in Figure 10.

3.2.3 Improving the interfacial properties of CO_2 foam

The properties of the gas-liquid interface strongly affect foam performance. The CO_2 foam stability will change with the variation of the interface properties. To analyze the mechanism underlying the synergistic effect of CTAB and SiO_2 nanoparticles on CO_2 foams, the interfacial properties of CTAB/SiO_2 dispersions and a pure CTAB solution at different concentrations were determined, as shown in Figure 12 and Figure 13.

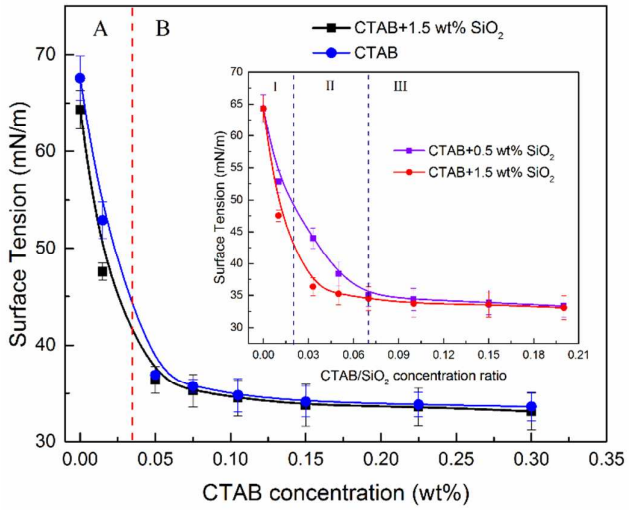

Figure. 12 Surface tension at different CTAB concentrations.

As shown in Figure 12, when the CTAB concentration was less than CMC (Region A in Figure 12), the surface tensions of the pure CTAB solution and the CTAB/SiO_2 dispersion with CO_2 rapidly decreased with the increase in the CTAB concentration. At the same CTAB concentration, the surface tension between the CTAB/SiO_2 dispersion and CO_2 was less than that between the pure CTAB solution and CO_2. When the CTAB concentration was higher than CMC (Region B in Figure 12), the two surface tensions essentially remained constant with the CTAB concentration and showed nearly the same values. At the same CTAB/SiO_2 concentration ratio, the interfacial tension between the dispersion and CO_2 decreased with an increase in the concentration of SiO_2 nanoparticles. When the CTAB concentration was greater than 0.1 wt%, CTAB molecules formed micelles in the solution and solubilized SiO_2 nanoparticles.[17, 22, 30, 31] The CTAB/SiO_2 dispersion looked like an emulsion. Most of the

nanoparticles remained in the bulk phase instead of the interface, and the surface tension between the dispersion and CO_2 was determined mainly by the surfactant.

When the CTAB concentration was 0, the surface tension of the 1.5 wt% SiO_2 dispersion was nearly the same as that of pure water, demonstrating that SiO_2 nanoparticles cannot reduce the surface tension, which is consistent with conclusions reported in the literature.[6, 12] Figure 12 shows that the surface tension of the CTAB/SiO_2 dispersion was less than that of pure CTAB solution and SiO_2 nanoparticles dispersion, particularly when the CTAB concentration was below CMC. The results are also consistent with conclusions reported in the literature.[35] This finding shows that SiO_2 nanoparticles and CTAB molecules produce a synergistic effect through which the surface-modified nanoparticles more easily adsorb onto the gas-liquid interface compared with pure CTAB molecules.[36] This effect reduces the difference in force between the gas and liquid phases at the interface such that the surface tension between the liquid and CO_2 is reduced, enhancing foaming capability and foam stability.

The interfacial viscoelastic modulus is usually used to describe the response of an interface to local contraction or expansion, reflecting the capability of a bubble film to resist deformation. Physically, this modulus refers to the change in surface tension with a change in unit surface area, as shown in equation (1). When an external disturbance at the interface or in the bulk phase near the interface results in a relaxation process, the interface will show viscoelastic properties. The greater the interfacial viscoelastic modulus of the liquid is, the higher the mechanical strength of the liquid film becomes and the more stable the bubble will be.[37]

$$\varepsilon = \frac{d\gamma}{d\ ln\ A} \tag{1}$$

where ε is the interfacial viscoelastic modulus, mN/m; γ is surface tension, mN/m; and A is surface area, m^2.

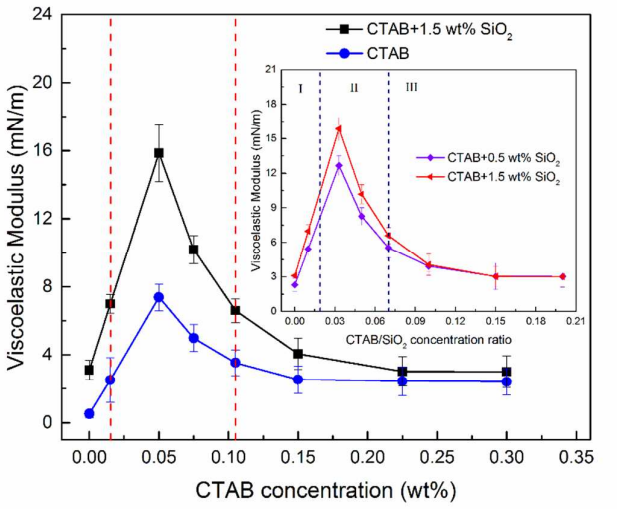

Figure. 13 Viscoelastic modulus at different CTAB concentrations.

As shown in Figure 13, the interfacial viscoelastic moduli of a pure CTAB solution and a CTAB/SiO_2 dispersion first increased and then decreased with an increase in the CTAB concentration, peaking at a CTAB concentration of 0.05 wt% or a concentration ratio of 0.033. Between 0.01 wt% and 0.105 wt% CTAB, the interfacial viscoelastic moduli were high, reflecting the higher strength of the bubble film. An increase in the surfactant bulk concentration can affect the interfacial viscoelastic modulus in two ways. Firstly, it can increase the surfactant concentration on the interface, which would cause higher interfacial tension gradient during the process of interface deforming, and a rising of the interfacial viscoelastic modulus. Increase of the interfacial viscoelastic modulus may play a dominant role when the CTAB concentration is less than 0.05 wt% in the experiment. Secondly, the rising surfactant bulk concentration can also increase the diffusing capability of the surfactant molecules from the bulk phase to a new interface when the CTAB concentration is greater than 0.05 wt%, which can decrease the interfacial tension gradient and the interfacial viscoelastic modulus remarkably.[38]

At a certain CTAB/SiO_2 concentration ratio, the modified SiO_2 nanoparticles can replace the CTAB molecules and adsorb onto the gas-liquid interface. Compared with CTAB, SiO_2 nanoparticles can more strongly increase the mechanical strength of the liquid film.[30-31] Figure 13 shows that, at the same CTAB concentration, the interfacial viscoelastic modulus of the CTAB/SiO_2 dispersion is much greater than that of the pure CTAB solution. At the optimal concentration ratio of 0.033, the interfacial viscoelastic modulus of the CTAB/SiO_2 dispersion can be up to twice that of the pure CTAB solution. Figure 13 also indicates that with an increase in the concentration of SiO_2 nanoparticles at the same concentration ratio, more nanoparticles can adsorb onto the gas-liquid interface, and the interfacial viscoelastic

modulus increases, enhancing the strength of the bubble film. However, the increase in the interfacial viscoelastic modulus of the film is much smaller than that in the nanoparticle concentration, indicating that the SiO_2 nanoparticles adsorbed onto the gas-liquid interface gradually reach saturation. When the saturation adsorption level is reached, a further increase in the SiO_2 nanoparticle concentration cannot improve the strength of the bubble film.

Figure 12 and Figure 13 show that, at a CTAB/SiO_2 concentration ratio of 0.033, the surface tension of the dispersion reached a small and stable value and the interfacial viscoelastic modulus reached its peak. At this concentration ratio, the number of CTAB molecules that adsorbed onto the nanoparticle surface was moderate; moreover, the nanoparticles were strongly hydrophobic, and the maximum number of nanoparticles could adsorb onto the gas-liquid interface. Under these conditions, the liquid film had a low interfacial energy and high strength, resulting in good foaming and stability performances. The results are consistent with those shown in Figure 3.

3.2.4 Reducing liquid discharge of CO_2 foam

Liquid discharge under gravity is another important factor affecting the stability of foams.[39] Under the action of gravity, the liquid is separated from bubbles, and bubble films gradually become thin and break. The liquid viscosity has a strong effect on liquid discharge. With an increase in the liquid viscosity, the liquid flow resistance increases, which greatly delays the process of liquid discharge.

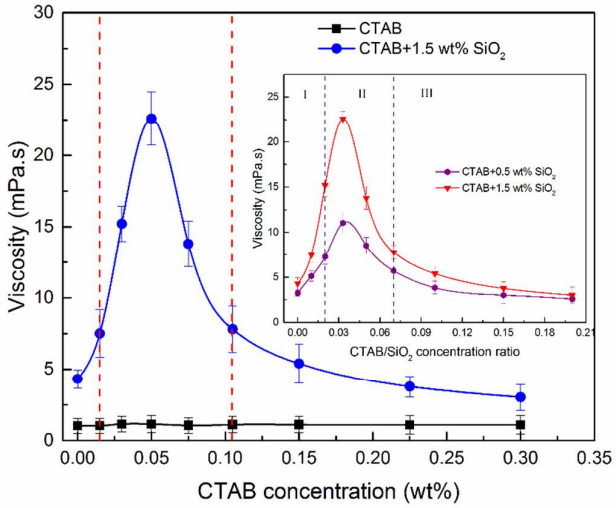

Figure. 14 The viscosity of CTAB/SiO_2 dispersion and pure CTAB solution at different CTAB concentrations (25□).

Under normal pressure and at 25 °C, the viscosity of the pure CTAB solution and that of the CTAB/SiO_2 dispersion were as shown in Figure 14. As indicated, the viscosity of the CTAB/SiO_2 dispersion was far higher than that of the pure CTAB solution in the CTAB

concentration range of 0.01 wt% to 0.1 wt%. At the optimum CTAB/SiO_2 concentration ratio of 0.033, the viscosity reached 23 mPa.s, approximately 20 times that of the pure CTAB solution at the same concentration. The dispersion reached such a high viscosity because SiO_2 nanoparticles formed a complex spatial structure due to the interaction of CTAB molecules adsorbed onto their surface shown in region C of Figure 8. In this region, a moderate amount of CTAB molecules adsorbed onto the surface of SiO_2 nanoparticles, forming a tight single adsorption layer or an incomplete double adsorption layer with proper electrostatic repulsion shown in Figures 6 and 7. The SiO_2 nanoparticles showed strong hydrophobicity. The particles greatly improved the viscosity and flow resistance of the liquid phase, delaying liquid discharge and increasing foam stability. With the further increase of the concentration ratio, the adsorbed SiO_2 nanoparticles formed a double-layer with the hydrophilic ends facing outwards, which strengthened the hydrophilicity of the nanoparticles and decreased the viscosity of the dispersion. Figure 14 also shows that the viscosity of the dispersion increased significantly with the concentration of SiO_2 nanoparticles at the same CTAB/SiO_2 concentration ratio. The reason is that at a higher concentration, SiO_2 nanoparticles would form a more complex spatial structure, increasing the flow resistance of the liquid.

With an increase in the CTAB/SiO_2 concentration ratio, the viscosity of the dispersion first increased and then decreased, which can be explained as follows. At low CTAB concentrations (less than 0.01 wt%), the ζ potential of the SiO_2 dispersion was low, and the nanoparticles existed in the agglomerated state in the CTAB solution; thus, the viscosity did not increase appreciably. When the CTAB concentration was too high (greater than 0.1 wt%), CTAB molecules formed micelles in solution and solubilized SiO_2 nanoparticles.[17, 22, 30, 31] The CTAB/SiO_2 dispersion looked like an emulsion. The flow resistance of the liquid phase was greatly reduced, and the macroscopic viscosity decreased.

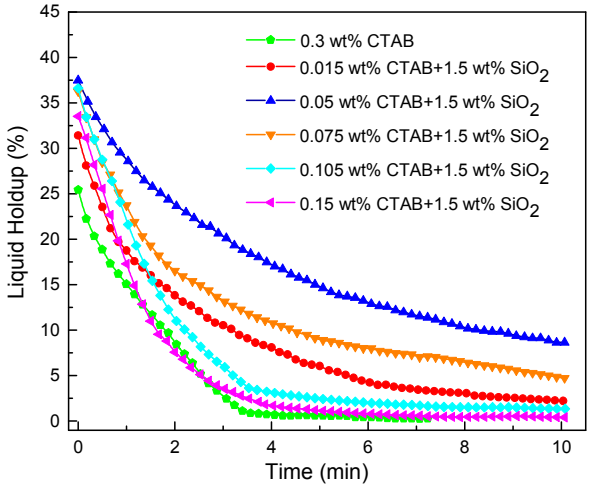

Figure. 15 The liquid holdup of CO_2 foams at different CTAB/SiO_2 concentration ratios.

The liquid holdup of CO_2 foams prepared using dispersions with different CTAB/SiO_2 concentration ratios is shown in Figure 15. The liquid holdup is determined with Equation (2) by foam volume, total liquid volume, and residual liquid volume separated out of the foam. The foam volume and residual liquid volume are measured with time by the Foamscan with the procedures mentioned previously.

$$f = \frac{V_{\mathrm{tl}} - V_{\mathrm{rl}}}{V_{\mathrm{f}}} \quad (2)$$

where, f is the liquid holdup, %; V_{tl} is the total volume of dispersion to generate foam, ml; V_{rl} is the residual liquid volume separated out of the foam, ml; V_{f} is the foam volume, ml.

The slopes with concentration ratios of 0.02 and 0.07 are smaller than the others. The slope represents the drainage velocity of the foams. The smaller the slope is, the slower the foams drain. The decrease in the slopes resulted in a decrease in the drainage velocity of the CO_2 foams, in agreement with the experimental results shown in Figure 14.

3.3 CO_2 foam flow in porous media through visual flooding experiment

The visual flooding of a CTAB/SiO_2 foam is shown in Figure 16. Due to the high mobility ratio between water and crude oil, water formed a continuous channel through the crude oil. A substantial amount of residual oil was left on the pore surface as an oil film in a discontinuous state after water flooding (Figure 16 a), and oil recovery of water flooding was unfavorable. The foam had a higher injection pressure due to the Jamin effect, improving the sweep efficiency (Figure 16 b).[40-42] Furthermore, bubbles can strip the oil film off of the pore surface through the high friction generated when bubbles deform and pass through pores (Figure 16 c), and surfactant molecules can also change the wettability of rock, allowing oil to move easily. At the end of foam flooding (Figure 16 d), most oil was recovered, and the oil recovery was greatly enhanced. Greater foam stability is usually related to higher oil recovery factor. Mobility of gas is much higher than that of other fluids in the reservoir, due to its low viscosity. However, foam can effectively decrease gas mobility and gas channeling under reservoir conditions, because continuous gas phase is separated by bubbles. The bubbles film with greater strengthen can improve foam stability and foam viscosity, which can improve the oil recovery.

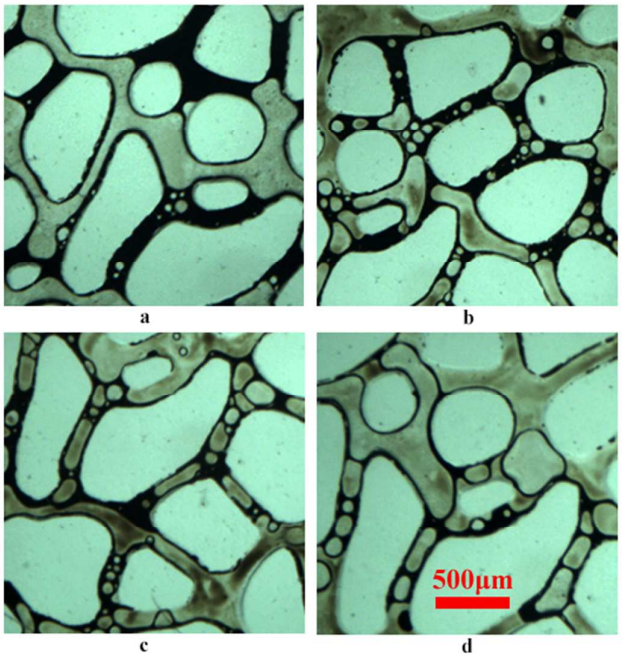

Figure. 16 Images of visual flooding experiment. (a) is the end of water flooding. (b) - (d) are CO_2 foam floodings at 1, 2, and 3 PV, respectively. The black areas in the visual model are crude oil, the small white bubbles are CO_2 foam prepared by CTAB/SiO_2 dispersion, and the large white areas are sand grains.

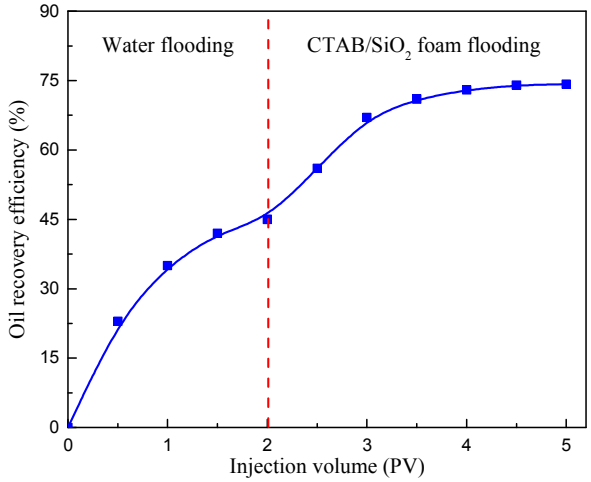

Figure. 17 Oil recovery efficiency at different injection volumes.

The curve of oil recovery efficiency for water flooding and subsequent CTAB/SiO_2 foam flooding is shown in Figure 17. Due to the high permeability of the visual model, water flooding had a better effect than that of a core or sandpack displacement experiment.[43-44] When the injection volume of water reached 2 PV, water channeling formed, and the oil recovery efficiency was approximately 45 %. At a high apparent viscosity and sweep coefficient, foam flooding can recover more residual oil trapped in pores. According to the

experiment results, the oil recovery efficiency reached 74.3 % at the end of foam flooding, demonstrating the favorable effects of CTAB/SiO_2 foams in EOR.

4. CONCLUSIONS

(1) The synergistic effects of CTAB/SiO_2 concentration ratios between 0.02 and 0.07 in stabilizing CO_2 foams were determined experimentally, and the optimal concentration ratio was 0.033. The optimal SiO_2 nanoparticle concentration was 1.5 wt%.

(2) The adsorption of CTAB molecules onto the surface of hydrophilic SiO_2 nanoparticles can be divided into two stages. In the first stage, the hydrophilic ends of the surfactant molecules adsorb onto the nanoparticle surface, and the hydrophobic ends are exposed, enhancing the hydrophobicity of the nanoparticles. In the second stage, more CTAB molecules adsorb onto the surface of the SiO_2 nanoparticles, forming a double adsorption layer and decreasing the hydrophobicity of the nanoparticles.

(3) With the increase in the CTAB/SiO_2 concentration ratio, the synergistic stabilization effect first increases and then decreases. The key factor is the adsorption of SiO_2 nanoparticles onto the gas-liquid interface. In the monolayer adsorption stage (concentration ratio from 0.02 to 0.033), as the concentration ratio increases, the hydrophobicity of the SiO_2 nanoparticles reinforces, the nanoparticles tend to adsorb onto the gas-liquid interface, and the stability of the CO_2 foam increases. In the double-layer adsorption stage (concentration from 0.033 to 0.07), with an increase in the concentration ratio, the hydrophobicity of the SiO_2 nanoparticles is reduced, the nanoparticles tend to exist in the bulk phase, and the stability of the CO_2 foam decreases.

(4) CTAB/SiO_2 dispersions stabilize CO_2 foams via three mechanisms. SiO_2 nanoparticles adsorbed at the interface can slow down the Ostwald ripening process. SiO_2 nanoparticles can improve the interfacial rheological properties and enhance the mechanical strength of the bubble film. Nanoparticles in the bulk phase can form a complex spatial structure, enhance the dispersion viscosity, and slow down liquid discharge. CTAB/SiO_2 foam can greatly improve oil recovery efficiency compared with water flooding.

AUTHOR INFORMATION

Corresponding Author

*E-mail: lsyupc@163.com for Songyan Li, and lizhm@upc.edu.cn for Zhaomin Li.

Notes

The authors declare no competing financial interest.

ACKNOWLEDGMENTS

This project was financially supported by the National Key Basic Research Program of China (No. 2015CB250904), the National Key Scientific and Technological Project for the Oil & Gas Field and Coalbed Methane of China (No. 2016ZX05011004-005), the National Natural Science Foundation of China (No. 51304229), and the Fundamental Research Funds for the Central Universities (14CX02185A). We are grateful to the Foam Research Center at the China University of Petroleum (East China) for their assistance with the experimental research.

REFERENCES

(1) Keller, K.; Yang, Z.; Hall, M.; Bradford, D. F. Carbon Dioxide Sequestration. Meanjin 2003, 19 (9), 881-883.

(2) Chung, F. T. H.; Jones, R. A.; Hai, T. N. Measurements and Correlations of the Physical Properties of CO_2 Heavy Crude Oil Mixtures. SPE Reserv. Eng. 1988, 3 (3), 822-828.

(3) Li, H. Z.; Zheng, S.; Yang, D. T. Enhanced Swelling Effect and Viscosity Reduction of Solvents-CO_2 Heavy Oil Systems. SPE J. 2013, 18 (4), 695-707.

(4) Holm, L. W. CO_2 Flooding: its Time Has Come. J. Petrol. Technol. 2013, 34 (12), 2739-2745.

(5) Jiang, H.; Shen, P.; Zhong, T.; An, X.; Qiao, W. The Relationship between CO_2 Storage and Oil Recovery Enhancing. Petrol. Geol. Recovery Effic. 2008, 15 (6), 52-55.

(6) Ma, K.; Liontas, R.; Conn, C. A.; Hirasaki, G. J.; Biswal, S. L. Visualization of Improved Sweep with Foam in Heterogeneous Porous Media Using Microfluidics. Soft Matter 2012, 8 (41), 10669-10675.

(7) Xie, S.; Yan, W.; Han, P. Mobility Control by Foam in CO_2 Flooding. Oilfield Chem. 1990, 7 (3), 289-294.

(8) Li, Z.; Sun, Q.; Li, S.; Zhang, N.; An, Z. Studies on Nanoparticles Improving the Stability of Foams. Oilfield Chem. 2013, 30 (4), 625-629.

(9) Yang, X. Application Status and Development Prospects of Nano Silicon Dioxide. Petrochemical Ind. Inner Mongolia 2011 (18), 26-27.

(10) Liu, J.; Zang, Y.; Wu, J.; Wang, M. The Development and Application of Nano Silicon Dioxide. J. Changchun University Technol. 2003, 24 (4), 9-12.

(11) Qiu-Feng, A. N.; Guo, K. Nano-SiO_2 Surface Modification and Research Progress of Application in Composite Materials. Nanosci. Nanotechnol. 2007, 29 (1), 157-158.

(12) Bi, Z.; Shi, Y.; Yan, W.; Yu, J. Adsorption of Cetyltrimethylammonium Bromide on Surface of Silicon Dioxide. Chem. Reagent 1997, 19 (6), 331-333.

(13) Tyrode, E.; Rutland, M. W.; Bain, C. D. Adsorption of CTAB on Hydrophilic Silica Studied by Linear and Nonlinear Optical Spectroscopy. J. American Chem. Soc. 2008, 130 (51), 17434-17445.

(14) Somasundaran, P.; Fuerstenau, D. W. Mechanisms of Alkyl Sulfonate Adsorption at the Alumina-water

Interface. J. Phys. Chem. 1966, 70 (1), 90-96.

(15) Santini, E.; Krägel, J.; Ravera, F. Study of the Monolayer Structure and Wettability Properties of Silica Nanoparticles and CTAB Using the Langmuir Trough Technique. Colloids Surf. A 2011, 382 (1), 186-191.

(16) Ravera, F.; Ferrari, M.; Liggieri, L.; Loglio, G.; Santini, E.; Zanobini, A. Liquid–liquid Interfacial Properties of Mixed Nanoparticle–surfactant Systems. Colloids Surf. A 2008, 323 (1-3), 99-108.

(17) Zhang, S.; Lan, Q.; Liu, Q.; Xu, J.; Sun, D. Aqueous Foams Stabilized by Laponite and CTAB. Colloids Surf. A 2008, 317 (1-3), 406-413.

(18) Kam, S. I.; Rossen, W. R. Anomalous Capillary Pressure, Stress, and Stability of Solids-coated Bubbles. J. Colloid Interf. Sci. 1999, 213 (2), 329-339.

(19) Fujii, S.; Ryan, A J.; Armes, S. P. Long-range Structural Order, Moiré Patterns, and Iridescence in Latex-stabilized Foams. J. American Chem. Soc. 2006, 128 (24), 7882-7886.

(20) Sethumadhavan, G. N.; Nikolov, A. D.; Wasan, D. T. Stability of Liquid Films Containing Monodisperse Colloidal Particles. J. Colloid Interf. Sci. 2001, 240 (1), 105-112.

(21) Nikolov, A. D.; Wasan, D. T. Dispersion Stability Due to Structural Contributions to the Particle Interaction as Probed by Thin Liquid Film Dynamics. Langmuir 1992, 8 (12), 2985-2994.

(22) Liu, Q.; Zhang, S.; Sun, D.; Xu, J. Foams Stabilized by Laponite Nanoparticles and Alkylammonium Bromides with Different Alkyl Chain Lengths. Colloids Surf. A 2010, 355 (1-3), 151-157.

(23) Worthen, A. J.; Parikh, P. S.; Chen, Y.; Bryant, S. L.; Huh, C.; Johnston, K. P. Carbon Dioxide-in-water Foams Stabilized with a Mixture of Nanoparticles and Surfactant for CO_2 Storage and Utilization Applications. Energy Procedia 2014, 63, 7929-7938.

(24) Martine, M. J.; Ruiz-Henestrosa, V. M. P.; Sánchez, C. C.; Patino, J. M. R.; Pilosof, A. M. R. Interfacial and Foaming Interactions between Casein Glycomacropeptide (CMP) and Propylene Glycol Alginate. Colloids Surf. B 2012, 95, 214-221.

(25) Boos, J.; Drenckhan, W.; Stubenrauch, C. Protocol for Studying Aqueous Foams Stabilized by Surfactant Mixtures. J. Surf. Deterg. 2013, 16, 1-12.

(26) Ravera, F.; Santini, E.; Loglio, G.; Ferrari, M.; Liggieri, L. Effect of Nanoparticles on the Interfacial Properties of Liquid/liquid and Liquid/air Surface Layers. J. Phys. Chem. B 2006, 110, 19543-19551.

(27) Cao, X. L.; Li, Y.; Jiang, S. X.; Sun, H .Q.; Cagna, A.; Dou, L. X. A Study of Dilational Rheological Properties of Polymers at Interfaces. J. Colloid Interf. Sci. 2004, 270, 295-298.

(28) Wang, Q.; Xi, H.; Zuo, Y. Review on Measurement Techniques of Performance and Influence Factors of Stability for Foam. J. Chem. Ind. Eng. 2007, 28 (2), 25-28.

(29) Liu, T.; Guo, R.; Shen, M.; Yu, W. Determination of the Diffusion Coefficients of Micelle and the First CMC and Second CMC in SDS and CTAB Solution. Acta Physico-chemical Sinica, 1996, 12 (4), 337-340.

(30) Li, S. Y.; Li, Z. M.; Wang, P. Experimental Study of the Stabilization of CO_2 Foam by SDS and Hydrophobic Nanoparticles. Ind. Eng. Chem. Res. 2016, 55, 1243-1253.

(31) Zhang, S.; Sun, D.; Dong, X.; Li, C.; Xu, J. Aqueous Foams Stabilized with Particles and Nonionic

Surfactants. Colloids Surf. A 2008, 324(1-3), 1-8.

(32) Young, T. An Essay on the Cohesion of Fluids. Philosophical Transactions of the Royal Society of London, 1805, 95, 65-87.

(33) Annable, T.; Buscall, R.; Ettelaie, R.; Shepherd, P.; Whittlestone, D. Influence of Surfactants on the Rheology of Associating Polymers in Solution. Langmuir, 2002, 10 (4), 1060-1070.

(34) Hunter, T. N.; Pugh, R. J.; Franks, G. V.; Jameson, G. J. The Role of Particles in Stabilizing Foams and Emulsions. Adv. Colloid Interf. Sci. 2008, 137 (2), 57-81.

(35) Sun, Q.; Li, Z.; Wang, J.; Li, S.; Li, B.; Jiang, L.; Wang, H.; Lü, Q.; Zhang, C.; Liu, W. Aqueous Foam Stabilized by Partially Hydrophobic Nanoparticles in the Presence of Surfactant. Colloids Surf. A 2015, 471, 54-64.

(36) Binks, B. P.; Horozov, T. S. Colloidal Particles at Liquid Interfaces: an Introduction in Colloidal Particles at Liquid Interfaces. Cambridge: Cambridge University. Press, 2006.

(37) Martin, D. F.; Taber, J. J. Carbon Dioxide Flooding. J. Petrol. Technol. 1992, 44 (4), 396-400.

(38) Wang, Y.; Zhang, L.; Sun, T.; Zhao, S.; Yu J. A Study of Interfacial Dilational Properties of Two Different Structure Demulsifiers at Oil-water Interfaces. J. Colloid Interf. Sci. 2004, 270, 163-170.

(39) Li, Y.; Zhao, G.; Zhang, P.; Chen, H.; Wang, A. Factors Affecting Foam Stability and Its Mechanism. Proceedings for Colloid and Interface Conference of Chinese Chemical Society, 2004.

(40) Li, S. Y.; Li, Z. M.; Li, B. F. Experimental Study on Foamed Gel Flow in Porous Media. J. Porous Media 2015, 18 (5), 519-536.

(41) Li, S. Y.; Li, Z. M.; Li, B. F. Experimental Study and Application of Tannin Foam for Profile Modification in Cyclic Steam Stimulated Well. J. Petrol. Sci. Eng. 2014, 118, 88-98.

(42) Li, S. Y.; Li, Z. M.; Li, B. F. Experimental Study and Application on Profile Control Using High-temperature Foam. J. Petrol. Sci. Eng. 2011, 78 (3-4), 567-574.

(43) Hirasaki, G. J.; Lawson, J. B. Mechanisms of Foam Flow in Porous Media: Apparent Viscosity in Smooth Capillaries. SPE J. 1985, 25 (2), 176-190.

(44) Li, S. Y.; Li, Z. M.; Lin, R. Y. Mathematical Models for Foam-diverted Acidizing and Their Applications. Petrol. Sci. 2008, 5 (2), 145-152.